Molecular Biology of the Cell
Vol. 10, 4299–4310, December 1999

Phosphorylated Human Keratinocyte Ornithine Decarboxylase Is Preferentially Associated with Insoluble Cellular Proteins

Mary M. Pomidor,* Rebecca Cimildoro,† Bien Lazatin,† Ping Zheng,‡§ James A. Gurr,•¶ Irene M. Leigh,# Olli A. Jänne,@ Rocky S. Tuan,*† and Noreen J. Hickok*†**

Departments of *Biochemistry and Molecular Pharmacology, †Orthopaedic Surgery, and ‡Dermatology, Thomas Jefferson University, Philadelphia, Pennsylvania 19107; •Department of Biochemistry, Temple University Medical School, Philadelphia, Pennsylvania 19140, #Academic Department of Dermatology, St. Bartholomew's and The Royal London School of Medicine and Dentistry, London, United Kingdom; and @Institute of Biomedicine, Departments of Physiology and Clinical Chemistry, University of Helsinki, Helsinki, Finland

Submitted August 18, 1999; Accepted October 8, 1999
Monitoring Editor: Paul T. Matsudaira

Ornithine decarboxylase (ODC), the first enzyme in polyamine biosynthesis, is highly regulated by many trophic stimuli, and changes in its levels and organization correlate with cytoskeletal changes in normal human epidermal keratinocytes (NHEK). NHEK ODC exhibits a filamentous perinuclear/nuclear localization that becomes more diffuse under conditions that alter actin architecture. We have thus asked whether ODC colocalizes with a component of the NHEK cytoskeleton. Confocal immunofluorescence showed that ODC distribution in NHEK was primarily perinuclear; upon disruption of the actin cytoskeleton with cytochalasin D, ODC distribution was diffuse. The ODC distribution in untreated NHEK overlapped with that of keratin in the perinuclear but not cytoplasmic area; after treatment with cytochalasin D, overlap between staining for ODC and for keratin was extensive. No significant overlap with actin and minimal overlap with tubulin filament systems were observed. Subcellular fractionation by sequential homogenizations and centrifugations of NHEK lysates or detergent and salt extractions of NHEK in situ revealed that ODC protein and activity were detectable in both soluble and insoluble fractions, with mechanical disruption causing additional solubilization of ODC activity (three- to sevenfold above controls). Fractionation and ODC immunoprecipitation from [^{32}P]orthophosphate-labeled NHEK lysates showed that a phosphorylated form of ODC was present in the insoluble fractions. Taken together, these data suggest that two pools of ODC exist in NHEK. The first is the previously described soluble pool, and the second is enriched in phospho-ODC and associated with insoluble cellular material that by immunohistochemistry appears to be organized in conjunction with the keratin cytoskeleton.

INTRODUCTION

Altered cell proliferation results from a complex series of events that include altered transcription of genes involved in cell cycle transit, e.g., proto-oncogenes c-myc, c-fos, and ornithine decarboxylase (ODC)[1], posttranscriptional events (Pawson, 1991), and altered cell shape because of a remodeled cytoskeleton (Li and Deshaies, 1993). We reported pre-

** Corresponding author. E-mail address: Noreen.Hickok@mail.tju.edu.
¶ Present addresses: Wyeth-Ayerst Research, Radnor, PA 19087;
§ Department of Neuroendocrinology, The Rockefeller University, New York, NY 10021.

Abbreviations used: α-DFMO, α-difluoromethylornithine; DMSO, dimethylsulfoxide; DOC, sodium deoxycholate; DTT, dithiothreitol; FITC, fluorescein isothiocyanate; KGM, keratinocyte growth medium; LDH, lactate dehydrogenase; NHEK, normal human epidermal keratinocytes; ODC, ornithine decarboxylase; P_0, initial pellet after lysis and ultracentrifugation; P_1, pellet resulting from homogenization of the P_0 pellet followed by ultracentrifugation; S_0, initial supernatant after lysis and ultracentrifugation; S_1, supernatant resulting from rehomogenization of the P_0 pellet and ultracentrifugation; TPA, 12-*O*-tetradecanoylphorbol-13-acetate; TRITC, tetramethylrhodamine isothiocyanate.

viously that agents that altered proliferation of normal human epidermal keratinocytes (NHEK) also caused reorganization of the actin cytoskeleton and of localization of ODC, an enzyme important for cell proliferation, suggesting that cellular architecture might influence ODC activity (Pomidor *et al.*, 1995).

ODC is the first enzyme in the biosynthesis of polyamines, cations important for many cellular processes, including chromatin condensation, and protein synthesis (Marton and Morris, 1987). Polyamines alter actin polymerization rates in vitro (Oriol-Audit *et al.*, 1985), and polyamine starvation results in gross cytoskeletal alterations in yeast and Chinese hamster ovary polyamine auxotrophs (Pohjanpelto *et al.*, 1981; Balasundaram *et al.*, 1991). Furthermore, cytoskeletal disrupters modulate ODC regulation by 12-*O*-tetradecanoylphorbol-13-acetate (TPA) and nerve growth factor (O'Brien *et al.*, 1976; Lakshmanan, 1979).

ODC overexpression has been shown to cause cellular transformation (Auvinen *et al.*, 1992; Moshier *et al.*, 1993) and hyperphosphorylation of $p130^{CAS}$, which is involved in cell transformation (Hölttä *et al.*, 1993; Auvinen *et al.*, 1995). Recently, rapid activation of ODC in transformed rat fibroblastic cells has been shown to be associated with phosphorylation of ODC accompanied by membrane localization (Heiskala *et al.*, 1999).

Together, these observations suggest that cell shape changes transduced via the cytoskeleton could regulate ODC and that altered ODC activity could influence actin organization and cell shape. We reported recently that cytoskeletal remodeling changed ODC localization and that suppression of ODC activity led to altered cytoskeletal architecture (Pomidor *et al.*, 1995). This regulated ODC distribution was especially intriguing with respect to ODC's role in cell transformation, because c-myc (Alexandrova *et al.*, 1995) and p53 (Maxwell *et al.*, 1991) can localize to the tubulin network.

We therefore have asked whether changes in ODC localization and cellular architecture occur concomitantly because ODC associates with a cytoskeletal protein complex. If this were the case, upon subcellular fractionation, ODC distribution would correlate with that of the cytoskeletal component(s). In this report, we present evidence by both double immunofluorescence and subcellular fractionation that there are two pools of ODC protein in NHEK. One of these is extracted with the soluble cellular material; the other fractionates with the insoluble material and, by immunofluorescence, appears to associate with keratin. Furthermore, the insoluble ODC appears to be enriched in the phosphorylated form of ODC and rendered inactive while insoluble. These data suggest how a cell could quickly activate ODC upon mitogenic stimulation.

MATERIALS AND METHODS

Materials

L-[1-^{14}C]Ornithine (40–60 mCi/mmol), [^{35}S]methionine (1000 mCi/mmol), and [^{32}P]orthophosphate (1–60 mCi/mmol) were from DuPont–New England Nuclear (Boston, MA) or Amersham (Arlington Heights, IL) with equivalent results. TPA, cytochalasin D, fluorescein isothiocyanate (FITC)- or tetramethylrhodamine isothiocyanate (TRITC)-conjugated secondary antibodies, rabbit anti-actin, mouse anti-monomeric and polymerized tubulin, and a monoclonal antibody panel to bovine hoof keratin were from Sigma (St. Louis, MO). Rhodamine–phalloidin was from Molecular Probes (Eugene, OR). Polyclonal rabbit antiserum to mouse ODC (cross-immunoreactive with human ODC [Leinonen *et al.*, 1987]) has been characterized previously (Isomaa *et al.*, 1983). Furthermore, we have published previously the equivalence of staining for ODC using this polyclonal antibody with a commercially available monoclonal antibody to murine ODC (Pomidor *et al.*, 1995). The mouse monoclonal antibody to human keratin 14 has also been described previously (LL001 [Sexton *et al.*, 1993]).

Cell Culture

NHEK and human dermal fibroblasts were established from neonatal foreskins as described previously and cultured in keratinocyte growth medium (KGM; BioWhittaker/Clonetics, Walkersville, MD) supplemented with 50 μg/ml bovine pituitary extract or DMEM supplemented with 10% newborn calf serum, respectively (Pomidor *et al.*, 1995). Treatments were initiated in fresh medium containing the agent or vehicle alone (100 ng/ml TPA, ethanol; 5 mM α-difluoromethylornithine [α-DFMO], PBS; 1 μg/ml cytochalasin D, dimethylsulfoxide [DMSO]; vehicle concentration $\leq$ 0.1% [vol/vol]). All procedures using human "surgical waste" were approved by the Institutional Review Board of Thomas Jefferson University.

In metabolic-labeling experiments, for [^{35}S]methionine labeling, NHEK were incubated in methionine-free KGM for 30 min and then methionine-free KGM containing 100 μCi/ml [^{35}S]methionine for 18 h at 37°C; for [^{32}P]orthophosphate incubations, NHEK were incubated in phosphate-free KGM for 30 min and then phosphate-free KGM containing 100 μCi/ml [^{32}P]orthophosphate for 3 h at 37°C. Incorporated counts in all labeling experiments were determined by trichloroacetic acid precipitation.

P0 HeLa cells (Staugaitis *et al.*, 1990) (kind gift of David Colman, Mt. Sinai School of Medicine, New York, NY) were cultured in DMEM containing 10% newborn calf serum. Expression of P0, a neural adhesion molecule, causes keratin filament organization and was induced by incubation with 0.5 mg/ml sodium butyrate for 24 h.

Immunofluorescent Localization

Fixed and permeabilized NHEK (Pomidor *et al.*, 1995) were incubated with ODC antibody (1:1000), human tubulin antibody (1:1000), or mouse monoclonal keratin-14 antibody LL001 (no dilution) in PBS containing 1% BSA for 30 min at 25°C, incubated with FITC- or TRITC-labeled secondary antibody, mounted using Fluoromount-G (Molecular Probes), and observed with epifluorescence using an Olympus BH-2 microscope or by laser confocal microscopy using the Odyssey Intervision System (Noran Instruments, Middleton, WI).

Labeling of Actin with Rhodamine–Phalloidin

Polymerized actin was stained by incubation with 2 μg/ml rhodamine–phalloidin for 30 min at 37°C (Dejana *et al.*, 1987). When cells were double-stained, they were first incubated with ODC antibody, followed by rhodamine–phalloidin.

Cell Fractionation I

NHEK at ~60% confluence were lysed by incubation with 10 mM Tris-HCl, pH 7.4, 10 mM NaCl, 1.5 mM $MgCl_2$, 0.3 M sucrose, and 0.5% Triton X-100 (vol/vol), at 4°C for 2 min (Soluble, Triton X-100 fraction), and residual soluble material was removed by rinsing with 10 mM Tris-HCl, pH 7.4, 10 mM NaCl, and 1.5 mM $MgCl_2$, at 4°C for 30 s (Wash) (Lenk *et al.*, 1977). The remaining cellular material was scraped into 10 mM Tris-HCl, pH 7.4, 10 mM NaCl, 1.5 mM $MgCl_2$, 1.0% Tween 20 (vol/vol), and 0.5% sodium deoxycholate (wt/vol; DOC), vortexed 30 s, and microcentrifuged 2 min (supernatant = DOC/Tween 20 fraction). The pellet was resus-

pended by pipetting in 10 mM Tris-HCl, pH 7.4, 500 mM NaCl, and 50 mM $MgCl_2$, incubated 2 min at 25°C, and microcentrifuged 2 min at room temperature (supernatant = High-Salt fraction). The pellet, containing insoluble material, was resuspended by pipetting in Triton X-100 buffer (Insoluble Pellet). The DOC/Tween 20 and high-salt fractions were diluted approximately eightfold and concentrated in Centricon-30 columns, 5000 × *g*, at 4°C for 60 min (Amicon, Beverly, MA). Before ODC activity assays, dithiothreitol (DTT) was added to a final concentration of 5 mM. In [^{32}P]orthophosphate-labeled cells, 1 mM sodium orthovanadate was included in buffers to inhibit phosphatases; all fractions were also treated with 1 U RNase and 1 U DNase for 30 min at room temperature to remove ^{32}P-labeled nucleic acids.

Cell Fractionation II

NHEK cultured to ~60% confluence were trypsinized, lysed by three freeze–thaw cycles in 25 mM Tris-HCl, pH 7.4, 0.1 mM Na_2EDTA, and 5 mM DTT (ODC buffer), and centrifuged at 150,000 × *g* at 4°C for 33 min (supernatant = soluble fraction S_0). The pellet (P_0) was homogenized by 40 strokes of a Dounce homogenizer (pestle B) in 25 mM Tris-HCl, pH 7.4, 0.1 mM Na_2EDTA, and 50 μM DTT with or without 2 mM sodium vanadate, incubated 1 h at 4°C, and centrifuged at 150,000 × *g* at 4°C for 33 min (supernatant from rehomogenization = S_1). The pellet (P_1) was resuspended by 40 strokes of a Dounce homogenizer in ODC buffer. Before activity assays, DTT was added to S_1 to a final concentration of 5 mM.

Lactate Dehydrogenase (LDH) Activity

LDH activity, a marker of soluble proteins, was measured in all fractions (LDL10 kit; Sigma). Those fractions containing LDH activity were considered to contain soluble proteins.

Protein Concentrations

Protein concentrations were determined for all fractions using the Bio-Rad protein assay kit (Richmond, CA).

Western Blotting

Equal volumes of fractions were boiled 3 min in SDS-sample buffer (66 mM Tris-HCl, 30% glycerol, 1% SDS, 5% β-mercaptoethanol, pH 6.8) and fractionated on a 10% SDS-polyacrylamide/4% stacking gel. Proteins were electrophoretically transferred to nitrocellulose (Schleicher & Schuell, Keene, NH), blocked for 2 h with 5% milk (wt/vol, Carnation, Nestlé USA, Solon, OH) in 10 mM Tris-HCl, pH 8.0, 150 mM NaCl, and 0.05% Tween 20 (vol/vol), and incubated with specific antiserum. After washing in 10 mM Tris-HCl, pH 8.0, 150 mM NaCl, and 0.05% Tween 20 (vol/vol), signal was visualized using alkaline phosphatase activity with 5-bromo-4-chloro-3-indolyl phosphate/nitroblue tetrazolium as substrate (ProtoBlot AP kit; Promega, Madison, WI). Western blotting to detect keratin used the monoclonal antibody panel to bovine hoof keratin.

ODC Activity

ODC activity was measured by the $^{14}CO_2$-release assay, using a final ornithine concentration of 0.5 mM (Seely and Pegg, 1983). Background $^{14}CO_2$ release was determined in the presence of the ODC inhibitor α-DFMO (a kind gift of Marion-Merrell Dow Research Institute, Cincinnati, OH) and subtracted from the activity. ODC activity was calculated as nanomoles of CO_2 per hour per milligram of protein and expressed as a percentage of control values on the basis of this calculation. The significance of differences between means was determined using the Student's *t* test for unpaired data.

ODC Immunoprecipitation and Protein Fractionation

Nonspecific immune complexes were removed by incubation of metabolically labeled NHEK fractions with 4 μl of rabbit preimmune serum in 150 mM NaCl, 5.0 mM EDTA, and 50 mM Tris-HCl, pH 7.4 (immunoprecipitation buffer; volume = 450 μl) for 24 h at 4°C, followed by pelleting with formaldehyde-fixed *Staphylococcus aureus* cells (0.7% final concentration; Calbiochem, Cambridge, MA). The cleared supernatant was immunoprecipitated with 3 μl of rabbit anti-mouse ODC (Isomaa *et al.*, 1983) for 12 h at 4°C, pelleted with *S. aureus* cells, and washed three times in immunoprecipitation buffer containing 0.5% NP-40 (vol/vol), 0.1% SDS (wt/vol), and 0.5% DOC (wt/vol). Dried pellets were resuspended in SDS sample buffer and fractionated on a 10% SDS-PAGE gel, and labeled proteins were visualized by autoradiography or a PhosphorImager (Molecular Dynamics, Sunnyvale, CA); band intensities were determined by the ImageQuant program (Molecular Dynamics).

Software for Image Reproduction

All blots and micrographs were reproduced and/or assembled using the Adobe Photoshop and Adobe Illustrator packages (Adobe Systems, San Jose, CA).

RESULTS

To investigate the basis for subcellular ODC distribution in NHEK, a two-pronged approach was chosen: 1) immunofluorescence microscopy to investigate whether ODC colocalized to a cytoskeletal filament system and 2) subcellular fractionation to determine the distribution of ODC protein in NHEK.

Immunofluorescent Localization of ODC

Because ODC localization appeared to change in concert with changes in cytoskeletal architecture (Pomidor *et al.*, 1995), we first asked whether ODC as visualized by immunohistochemistry colocalized with immunofluorescently labeled NHEK actin, tubulin, or keratin filament systems. NHEK double-immunostained for cytoskeletal components and ODC were optically sectioned by laser confocal microscopy on the fluorescein (ODC) and rhodamine (cytoskeletal component) channels, and images from the same section were superimposed (Figure 1). In all fields, ODC had a nuclear/perinuclear localization with faint, filamentous cytoplasmic staining (Figure 1, B, E, and H), except in one cell undergoing mitosis (Figure 1E) that had diffuse staining.

Actin staining was comprised of a thick semicircular band of filaments with radial microspikes, suggesting cell spreading (Figure 1). Superposition of the actin and ODC fields (Figure 1C) showed few areas of overlap (green over red = yellow), suggesting that ODC did not colocalize with the actin microfilament system.

The microtubule network (Figure 1D) consisted of fine filaments radiating throughout the cell as well as a perinuclear band; the mitotic cell had short microtubules. Superposition of the ODC and tubulin images (Figure 1, E and D, respectively) showed minimal overlap in the perinuclear region (Figure 1F, yellow), suggesting that they did not significantly colocalize.

The keratin intermediate filament network (Figure 1G) appeared perinuclear with filaments radiating outward to form a fine meshwork. Superposition of the keratin and ODC images (Figure 1I) showed overlap in the NHEK pe-

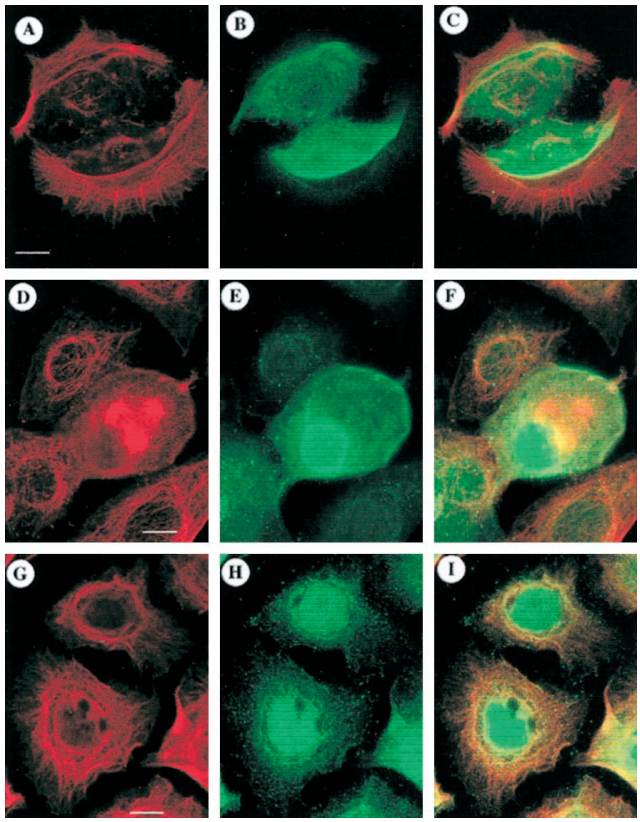

Figure 1. ODC and cytoskeletal organization in normal human epidermal keratinocytes. To assess potential colocalization of ODC with a cytoskeletal component, NHEK were stained for ODC (B, E, or H) and actin (A), tubulin (D), or keratin (G) and optically sectioned using confocal laser-scanning microscopy, and corresponding images were superimposed to determine the degrees of overlap (C, F, or I; orange-yellow→yellow). Superposition of actin (A) with ODC (B) showed little overlap (C) of the two staining patterns. Tubulin (D) and ODC (E) staining showed little overlap (F) except in a cell undergoing mitosis in which staining was apparent throughout. Keratin (G) and ODC (H) exhibited overlap (I) in the perinuclear region of the cell with little overlap outside of that region. Digital micrographs were collected using the Noran Intervision software (Noran Instruments). Bars: A–C, D–F, and G–I, 10 μm.

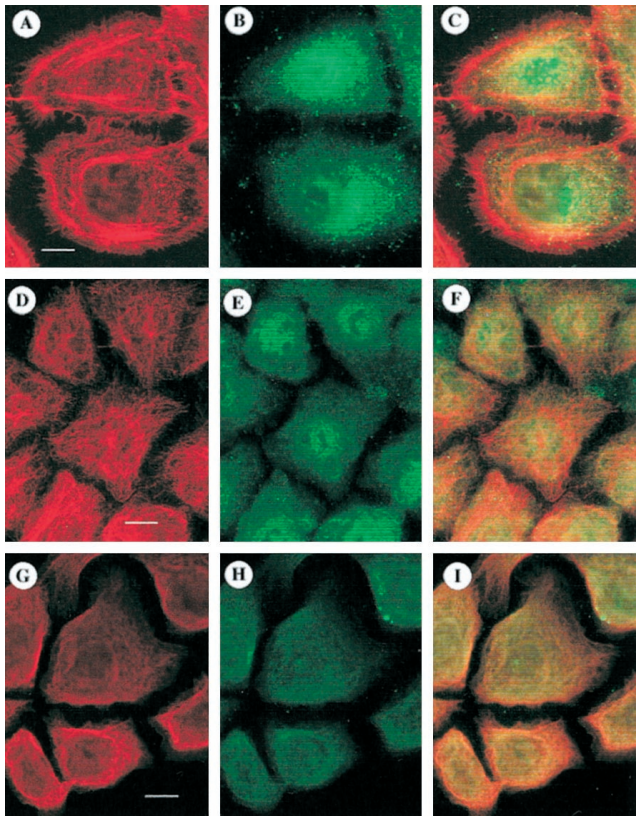

Figure 2. ODC and cytoskeletal organization in cytochalasin D–treated NHEK. To determine the effects of remodeling the cytoskeleton on ODC organization, NHEK were treated with 1 μg/ml cytochalasin D for 6 h, stained for ODC (B, E, or H) and actin (A), tubulin (D), or keratin (G), and optically sectioned by confocal laser-scanning microscopy, and corresponding images were superimposed to determine the degrees of overlap (C, F, or I; orange-yellow). Superposition of actin (A) with ODC (B) showed only minimal areas of overlap (C). Tubulin (D) and ODC (E) staining showed nonspecific areas of overlap (F). Keratin (G) and ODC (H) exhibited extensive overlap throughout the cells (I). Bars: A–C, D–F, and G–I, 10 μm.

rinuclear region (bright yellow), with some overlap with the cytoplasmic keratin meshwork (orange-yellow). We also examined the localization of ODC in NHEK that had been grown in 2.2 mM Ca^{2+}, one of the signals that induces NHEK differentiation. In NHEK that expressed K10, a suprabasal keratin, ODC distribution was diffuse (our unpublished results). Thus, it seemed that the best candidate for colocalization of ODC would be the NHEK keratin, specifically K14, network. No significant colocalization with microtubule or actin systems was observed.

We reported previously that the actin polymerization inhibitor cytochalasin D caused a more diffuse ODC distribution (Pomidor *et al.*, 1995). We reasoned that this changed-ODC localization could be caused by a specific cytoskeletal association that reflected the remodeling cytoskeleton. ODC staining in NHEK treated with 1 μg/ml cytochalasin D for 6 h was diffuse and comprised of fine filaments throughout the cell excluding the nucleoli (Figure 2, B, E, and H); the majority of stained actin was in microspikes, cell–cell contacts, or actin bundles (Figure 2A). Superposition (Figure 2C) of actin and ODC fields showed some intense yellow areas caused by superposition of ODC with short actin bundles. Little superposition of ODC was observed with actin filaments or microspikes, consistent with our conclusion that colocalization of ODC with the actin microfilament system is unlikely.

After cytochalasin D treatment, tubulin staining (Figure 2D) consisted of fine intersecting filaments. Superposition (Figure 2F) of tubulin and ODC fields showed some overlap in the nucleus (yellow), with green ODC staining throughout the cell. Thus, overlap between tubulin and ODC is most probably attributable to the diffuse ODC signal.

In cytochalasin D–treated NHEK, the keratin network (Figure 2G) appeared as dense, fine, interwoven filaments.

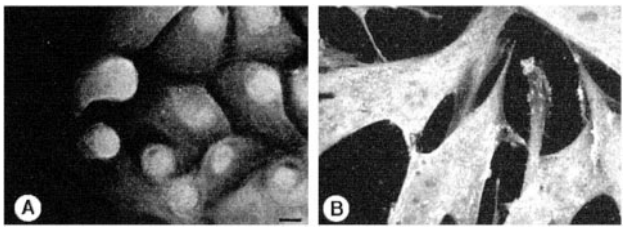

Figure 3. ODC localization in NHEK and in human dermal fibroblasts. To determine the effects of different cytoskeletal systems on ODC organization, NHEK (A) that contain a keratin intermediate filament system and fibroblasts (B) that contain a vimentin intermediate filament network were compared. The NHEK showed a predominately nuclear/perinuclear localization for ODC; the fibroblasts showed ODC staining throughout the cell. Digital micrographs were collected on a Bio-Rad confocal microscope. Bar, 10 μm.

Superposition (Figure 2I) of the ODC and keratin fields showed yellow areas throughout the NHEK; some areas with more intense keratin staining (orange→red) were observed in the cortical regions.

In summary, ODC appeared to colocalize significantly with the cytochalasin D–treated NHEK keratin intermediate filament system. Taken together with the data in Figure 1, these stainings suggested that a subset of ODC colocalized with the keratin intermediate filament system.

ODC Localization in Cells Not Containing Keratin

If the subcellular distribution of ODC not only correlated with but was dependent on a keratin intermediate filament network, then a cell that lacked keratin, such as the fibroblast, would show a markedly different ODC organization. We therefore compared ODC staining in human dermal fibroblasts and in NHEK. In contrast to the nuclear/perinuclear staining seen in NHEK (Figure 3A), ODC staining was diffuse throughout the human dermal fibroblasts, excluding the nucleoli (Figure 3B). Therefore, the presence of the keratin filament system correlated with a nuclear/perinuclear localization for ODC.

ODC Localization in P0 HeLa Cells

Finally, we reasoned that if we could induce the keratin filament system to remodel, then ODC should concomitantly relocalize. We therefore examined a stably transfected line of HeLa cells that can be induced by butyrate to express the neural adhesion molecule P0 (Staugaitis *et al.*, 1990); P0 expression causes keratin filament organization. Double immunolabeling showed that untreated P0 cells that express little P0 are small with little apparent keratin organization (Figure 4A) and have diffuse ODC staining (Figure 4B). After butyrate treatment, P0 expression is increased (Staugaitis *et al.*, 1990); the cells become larger and display a keratin filament network with strong perinuclear staining (Figure 4C), while ODC staining (Figure 4D) is filamentous with some distinct perinuclear localization. These observations further support a dependence of ODC localization on keratin intermediate filament organization.

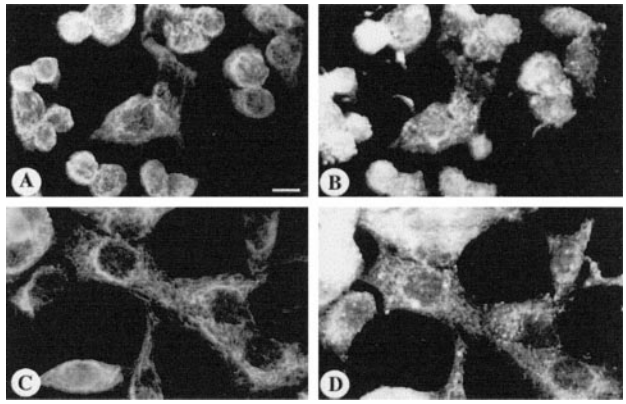

Figure 4. Keratin (A and C) and ODC (B and D) organization in P0 HeLa cells. Cells from a clone of HeLa cells that can be induced to express the neural adhesion molecule P0 were small and round, with short, disorganized keratin filaments (A) and little apparent organization to the ODC staining (B). After treatment with sodium butyrate, the cells became larger and more spread out, with a fine meshwork of keratin filaments (C); ODC staining had changed in parallel with keratin (D). Bar, 25 μm.

Subcellular Fractionation of NHEK by Detergent and Salt Extractions

The apparent colocalization of ODC with the keratin filament network suggests that some ODC activity should be associated with NHEK subcellular fractions containing insoluble proteins that include keratin. Previously, ODC activity was found only with soluble proteins (Seely *et al.*, 1982; Isomaa *et al.*, 1983), and recently a small percentage has been found to be localized to the plasma membrane after treatment with TPA (Heiskala *et al.*, 1999). Using a subcellular fractionation procedure (Lenk *et al.*, 1977) that solubilizes cellular proteins by detergent and salt extractions, we asked in what fractions ODC activity was measurable. Briefly, soluble proteins were collected in 0.5% Triton X-100 and a wash, membrane proteins and protein–protein complexes were solubilized in 1% Tween 20 and 0.5% DOC, additional protein–protein complexes were disrupted with 500 mM NaCl, and the remaining material that was enriched in keratin was considered insoluble (Lenk *et al.*, 1977). Analysis of equal volumes of each fraction showed that LDH activity, a soluble protein marker, was measurable solely in the Triton X-100 (Soluble) and wash fractions (Figure 5); therefore further detergent and salt treatments extracted proteins considered insoluble. ODC activity was detected in the soluble (Figure 5, histogram, Triton X-100 [Soluble] and Wash) and insoluble (Figure 5, histogram, Doc/T-20 and Ins Pellet) fractions. Therefore, soluble and insoluble pools of ODC activity were detected by subcellular fractionation.

We next asked, using this fractionation scheme, with what fractions did cytoskeletal components and a nuclear protein, pur α (Chang *et al.*, 1996), elute. Pur α was measured because we observed ODC in the nucleus in many micrographs; therefore, "insoluble" ODC activity could be caused by delayed lysis of the keratinocyte nucleus. Western blots showed that both actin and tubulin were extracted in the soluble fractions; keratins were present both in the soluble and insoluble pellet fractions (Figure 6). The nuclear protein

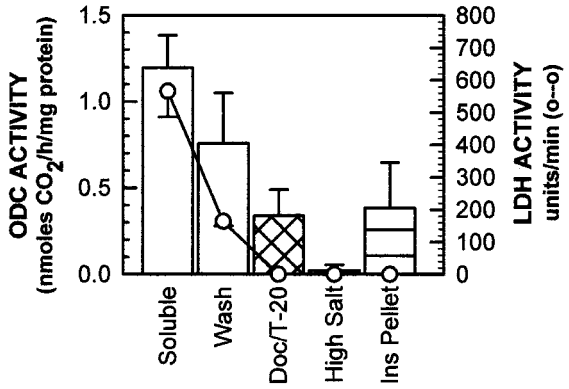

Figure 5. Subcellular fractionation of ODC activity. By the use of detergent and salt extractions, NHEK were fractionated (Lenk *et al.*, 1977), and fractions with high salt were dialyzed. LDH (open circles) activity was measured solely in the Soluble and Wash fractions. ODC activity (vertical bars) was measured in the Soluble and Wash fractions and also in the insoluble (Doc/T–20 and Ins Pellet) fractions. Data represent the average of measurements from three independent plates in one experiment. Similar results were obtained in many independent experiments. Doc/T-20, DOC and Tween 20; Ins, insoluble.

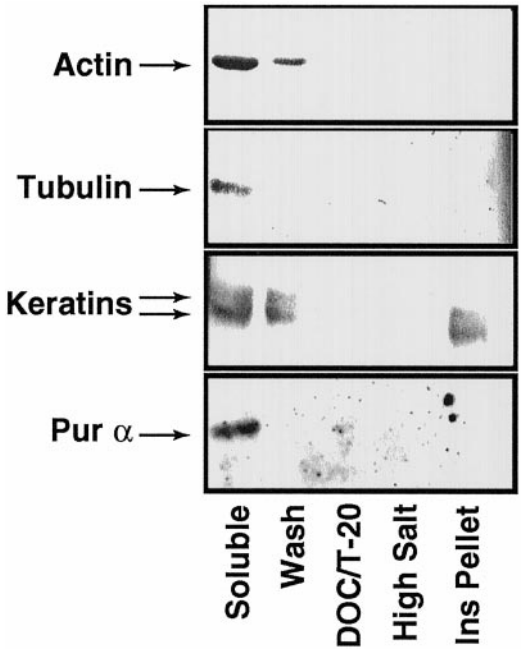

Figure 6. Western blots of lysates from subcellular fractions; determination of fractions containing different cytoskeletal components and nuclear proteins. By the use of detergent and salt solubilization of proteins (Lenk *et al.*, 1977), fractionated cell lysates were probed by Western blotting for actin, tubulin, keratins (monoclonal antibody to bovine hoof keratin), or pur α. Actin and tubulin were extracted in the Soluble fractions, keratin was extracted in the Soluble and Ins Pellet fractions, and pur α was extracted in the Soluble fraction.

pur α was present solely in the soluble fraction (Figure 6); in parallel, DNA was measured predominantly in the soluble fractions with small amounts in the insoluble pellet (our unpublished results). Taken together with the ODC activity measurements, the fractionation profiles indicated that in cellular fractions depleted of actin, tubulin, and nuclear proteins, significant ODC activity was present, suggesting that insoluble ODC activity was associated with insoluble proteins.

Immunoprecipitation of ODC from Subcellular Fractions

We and others have reported previously that TPA treatment causes decreased ODC levels in proliferating NHEK (Fischer *et al.*, 1993; Ruhl *et al.*, 1994). The subcellular distribution of ODC protein was therefore also determined by immunoprecipitation from fractionated, [^{35}S]methionine-labeled NHEK lysate that had been treated with or without TPA (Figure 7A). The immunoprecipitate from equal volumes of each fraction was fractionated by SDS-PAGE, and relative ODC levels were determined by fluorography. A band at the size of ODC was seen in all lanes at varying intensities (Figure 7A, arrow), and TPA treatment caused decreased ODC levels in all bands examined. The identity of the band at 52 kDa as ODC was confirmed by immunocompetition with bacterially expressed mouse ODC (kind gift of T. G. O'Brien, Lankenau Medical Center, Wynnewood, PA, or of L. Persson, University of Lund, Lund, Sweden) (our unpublished result).

Detection of Phospho-ODC

Ornithine decarboxylase has been reported to be phosphorylated on multiple sites (Rosenberg-Hasson *et al.*, 1991; Reddy *et al.*, 1996; Heiskala *et al.*, 1999). We therefore asked 1) where phosphorylated ODC partitioned in this subcellular fractionation scheme and 2) whether our previous observations on the effects of TPA on ODC levels in NHEK were reflected in changes in the levels of phosphorylated ODC because TPA activates protein kinase C. NHEK were treated with or without 100 ng/ml TPA for 6 h while being labeled with [^{32}P]orthophosphate (Figure 7B). Cells were fractionated; equal counts from each fraction were immunoprecipitated with ODC antibody, fractionated by SDS-PAGE, and visualized by autoradiography (Figure 7B). Three immunoprecipitated phosphoproteins were observed only in the Insoluble Pellet fraction, and all showed decreased phosphorylation after TPA treatment. The lowest protein band was of the size for ODC (~52,000 daltons), and the larger doublet was for phosphorylated keratin (confirmed by Western blotting; our unpublished results).

We then asked whether the keratin bands in the ODC immunoprecipitate resulted from a specific association of ODC with a keratin-containing protein complex. Keratin is primarily insoluble and can be pelleted by ultracentrifugation (Franke *et al.*, 1981). If association between ODC and keratin was specific, then pelleting of keratin would result in pelleting of ODC; if nonspecific, then the majority of ODC should remain in the supernatant. Therefore, lysates from each fraction were clarified by ultracentrifugation at 150,000 × *g* for 33 min, and the resultant supernatants were analyzed by ODC immunoprecipitation

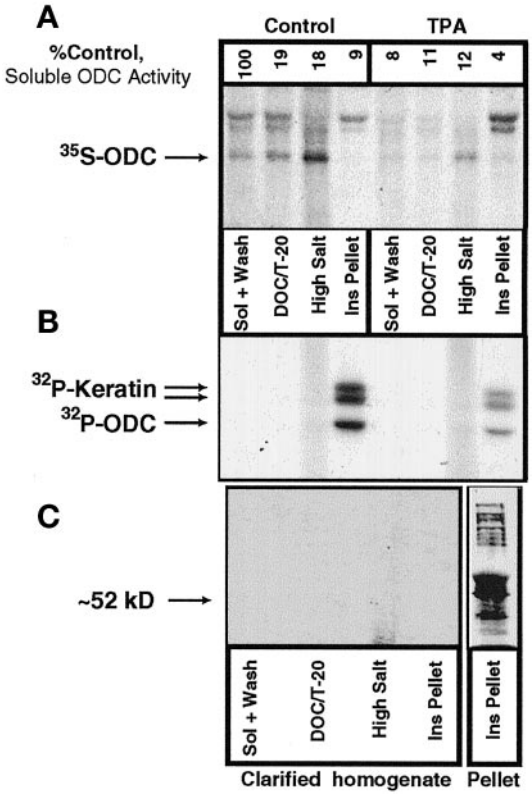

Figure 7. Subcellular fractionation of radiolabeled ODC. (A) [^{35}S]methionine-labeled NHEK lysate that had been treated with vehicle or 100 ng/ml TPA for 6 h was fractionated by detergent and salt extractions. Immunoprecipitable ODC protein was detectable in all fractions, with TPA treatment decreasing ODC levels, as we have reported previously (Ruhl *et al.*, 1994). (B) NHEK were then labeled with [^{32}P]orthophosphate and fractionated, and ODC was immunoprecipitated. Three bands were visible in the Ins Pellet fraction, one at the appropriate molecular size for ODC and the other two for keratins. (C) To determine whether the presence of the keratin bands was caused by specific interactions with ODC, the insoluble protein in the fractions was pelleted by ultracentrifugation, and ODC was immunoprecipitated from the resulting supernatant. No ODC was immunoprecipitated after this procedure. The lack of signal was not caused by degradation of the extract, as is shown in the Pellet column in which multiple phosphoproteins are apparent. Sol, soluble.

(Figure 7C). No immunoprecipitated phosphoproteins were visible by autoradiography in any lane (Figure 7C, Clarified homogenate panel). The lysate still contained ^{32}P-labeled proteins (Figure 7C, Pellet), indicating that ^{32}P-labeling had not been compromised. This pelleting of ODC was consistent with association of ODC with a keratin protein complex as had been suggested by the coimmunoprecipitation of ODC and keratin.

In summary, ODC protein could be detected in all subcellular fractions, with phosphorylated ODC detected only in the insoluble pellet. Therefore, it appeared that ODC was present as both a soluble and an insoluble protein, with the insoluble pool enriched in phospho-ODC.

Fractionation of NHEK Lysate by Sequential Centrifugation

During purification of ODC, it was reported to be a soluble protein (Seely *et al.*, 1982; Isomaa *et al.*, 1983), with the results we obtained above both confirming and extending this observation. To determine how the pools of ODC activity that we had described above compared with the results in the literature, we next examined the distribution of ODC using a procedure that mimics the first steps in the purification of the enzyme (Isomaa *et al.*, 1983). First, we examined the distribution of ODC activity in the supernatant and pellet of cells that had been lysed by three freeze–thaw cycles followed by ultracentrifugation. This measurement was performed to compare specifically the standard way of measuring ODC activity with the results obtained in the fractionation procedure described above. Furthermore, we asked whether resuspension of the 100,000 $\times$ *g* pellet in 2 mM orthovanadate and ODC buffer would alter ODC activity (Figure 8A), because we had noted that inclusion of the phosphatase inhibitor orthovanadate in the extraction buffers sometimes resulted in increased ODC activities. The ODC activity of the soluble fraction (S_0) was many times greater than that of the pellet (P_0), consistent with results reported by others for ODC purification (Isomaa *et al.*, 1983). LDH activity was measured and confirmed the assignment of the soluble and insoluble fractions (our unpublished results).

During the first fractionation procedure, cellular proteins that were not yet solubilized remained on the tissue culture plate (our unpublished results) or were pelleted in the later fractionation steps. Therefore, if a protein was interacting with ODC and causing reduced ODC activity, on the basis of the first subcellular fractionation scheme, we would expect this protein to have a solubility different from that of ODC. Therefore, cell lysates were separated (Figure 8, flow chart at top) into a supernatant (S_0) and pellet (P_0). The P_0 pellet was rehomogenized and centrifuged to yield an additional supernatant (S_1) and pellet (P_1). ODC activity was measured in all fractions and corrected for non-ODC decarboxylations by incubation with α-DFMO. Also, because activation of an ODC isozyme by GTP was reported (Hietala *et al.*, 1988), we asked whether insoluble ODC activity was sensitive to GTP. Whereas the P_0 pellet showed little activity, the S_1 supernatant showed three- to sevenfold greater specific activity, depending on the treatment, than did the S_0 supernatant (Figure 8B). In addition, in untreated samples, the separation into S_1 and P_1 resulted in significantly greater ODC activity in P_1, suggesting that additional ODC was released by resuspension of the P_1 pellet (Figure 8B). In parallel, LDH activity measurements in select fractions confirmed that soluble proteins were primarily concentrated in the S_0 supernatant, with little LDH activity measured in P_0, S_1, or P_1 (Figure 8B). These experiments suggested that, in addition to the ODC activity associated with soluble proteins, additional ODC was pelleted by centrifugation. The pool that associated with the insoluble fraction could be solubilized by homogenization, and treatments with neither vanadate nor GTP enhanced this effect, suggesting it was solely dependent on the repeated separations. Furthermore, because we measured much lower levels of ODC activity in P_0 than in S_1 and P_1, it suggested that the additional homogenization was somehow activating ODC or that the separation of the

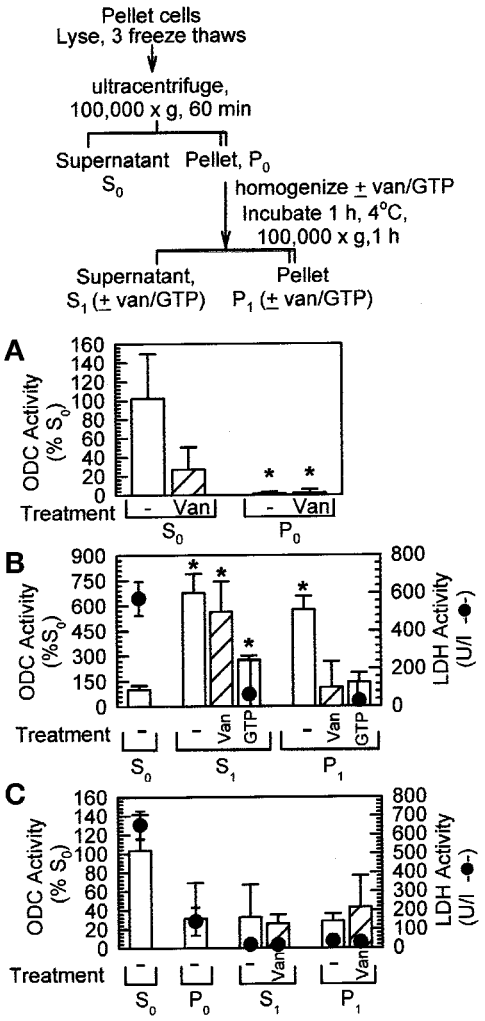

Figure 8. Fractionation of ODC activity by sequential homogenizations and centrifugations. (A) NHEK were lysed, and soluble protein was separated from insoluble protein by ultracentrifugation. The pellet was homogenized, and ODC activity (vertical bars) was measured (±2 mM orthovanadate [Van or van], a phosphatase inhibitor) using the $^{14}CO_2$-release assay. ODC activity was significantly greater in the supernatant (S_0) fractions than in the pellet (P_0) fractions. (B) The insoluble materials were again separated from the soluble materials after the P_0 homogenization (see flow chart at the top). From three to seven times the activity of the S_0 supernatant was measured in the S_1 supernatant; the P_1 pellet also showed considerable ODC activity. (C) In fibroblasts, ODC activity was greatest in the S_0 fraction, with all other manipulations resulting in activities approximately equivalent to that of the fibroblast P_0 pellet. Filled circles in B and C indicate LDH activity measured in parallel, indicating that soluble proteins were contained in the S_0 fractions. Data in A and B represent independent measurements of 3–10 individual plates from a single experiment; data in C represent the average of 4 individual plates from each of two independent experiments (n = 4–8). The results in A and B were reproduced in greater than two repeats of the individual parts of the experiments; for C, an additional experiment yielded similar results. *$p < 0.05$ (as compared with S_0 fractions).

proteins into these fractions was necessary for the detection of the additional activity.

Finally, we tested the subcellular distribution of ODC in fibroblasts that had showed no distinct subcellular localization of ODC by immunohistochemistry. This experiment was a means of testing the correlation between the organization of the ODC as observed by immunohistochemistry and the distribution as tested biochemically. We fractionated (see Figure 8, flow chart at top) fibroblasts and measured ODC activities in S_0, P_0, S_1, and P_1 (Figure 8C). The P_0 pellet had ~25% of the activity of the S_0 supernatant; further homogenization and separation into S_1 and P_1 did not result in additional ODC activity above that in P_0. Again, the majority of LDH activity was found in the S_0 fractions, with 6-to 10-fold less activity in P_0, S_1, and P_1, confirming that soluble proteins were released into S_0. Taken together, the data presented in Figure 8 identify a pool of ODC that is inactive in NHEK until further homogenization; this pool of ODC is not measured in fibroblasts, consistent with a dependence on proteins not shared between NHEK and fibroblasts, e.g., keratin.

Immunoprecipitation of ODC from Subcellular Fractions Obtained by Sequential Homogenizations and Centrifugations

The level of ODC activity measured in S_1 was high, suggesting that significant ODC protein levels should be present in S_1 and P_1. This was tested by immunoprecipitating ODC protein from the different fractions outlined in Figure 8. Equal counts of metabolically labeled ODC from each fraction were immunoprecipitated, fractionated by SDS-PAGE, and visualized by fluorography, and in parallel, actin, tubulin, and keratin were determined by Western blotting of unlabeled fractions. Figure 9 shows that a radiolabeled protein of the appropriate size for ODC was immunoprecipitated by the ODC antibody in all fractions. Actin was found in all fractions, tubulin was only in S_0, and keratin was only in P_1. The presence of ODC protein in each fraction supported the interpretation of the ODC activity measurements described in Figure 8.

DISCUSSION

Changes in cell shape are often causally linked to cell proliferation or differentiation via signals transduced through the cell surface (Schaller and Parsons, 1994). Many studies of the molecular mechanisms of proliferation have focused on the regulation of proteins necessary for cell cycle transit, such as myc, fos, p53, and cdc kinases, and altered cytoskeletal architecture to integrate ultimately signal transduction pathways with cytoskeletal changes (Pawson, 1991; Ingber *et al.*, 1995; Assoian and Zhu, 1997). In this article, we have focused on the subcellular distribution of the growth-regulatory enzyme ODC as visualized by immunohistochemistry and as measured in subcellular fractions. We have shown that its subcellular localization appears to depend on the NHEK keratin intermediate filament network and that the pool of ODC that is extracted with the insoluble material is more highly phosphorylated and shows attenuated activity levels until further fractionated from this insoluble material.

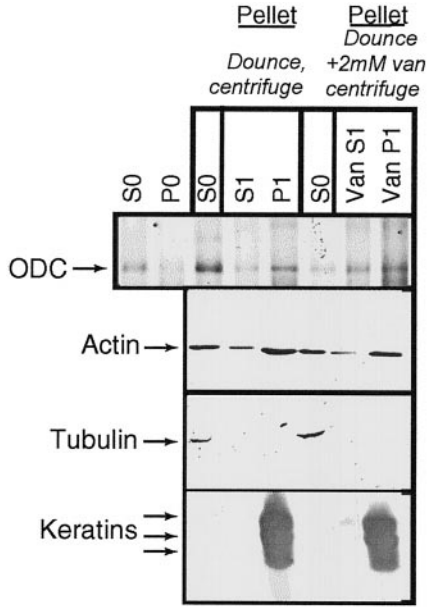

Figure 9. Fractionation of ODC protein and of cytoskeletal components. ^{35}S-labeled NHEK fractions were immunoprecipitated with ODC antibody or probed for actin, tubulin, or keratin by Western blotting, using the fractionation scheme detailed in Figure 8. ODC protein was present in all fractions, as was actin. Tubulin was found only in the S_0 fractions, with keratin only in the P_1 fractions.

Several of the characteristics of NHEK made them ideal for this study. For example, NHEK proliferation and differentiation are profoundly affected by changes in cell shape (Watt *et al.*, 1988; Adams and Watt, 1989), with signals that cause cytoskeletal remodeling also influencing adherence and migration, processes central to wound healing and skin development (Kubler *et al.*, 1991; Watt *et al.*, 1993). We showed previously that TPA treatment changes NHEK cytoskeletal organization and ODC subcellular localization. Interestingly, ODC subcellular localization appeared to be coordinately regulated with actin cytoskeletal organization because cytochalasin D, an actin polymerization inhibitor, and the ODC inhibitor α-DFMO caused a remodeling of the actin cytoskeleton and a concomitant relocalization of ODC (Pomidor *et al.*, 1995). Also, cytochalasin D and the microtubule depolymerizer colchicine abrogate induction of ODC (O'Brien *et al.*, 1976; Lakshmanan, 1979). Finally, a membrane localization for a pool of ODC has been associated with treatment of rat fibroblastic cells with TPA (Heiskala *et al.*, 1999). These studies taken together demonstrate that agents that change ODC localization also regulate ODC activity levels, suggesting a functional role for ODC localization.

In this study, we asked whether the observed coregulation of actin and ODC organization is caused by colocalization of ODC with a cytoskeletal component and investigated the biochemical basis for this phenomenon. We first examined by double immunofluorescence whether ODC colocalized with the actin, tubulin, or keratin filament networks in control and cytochalasin D–treated NHEK. Because cytochalasin D causes all NHEK cytoskeletal systems to remodel, we reasoned that if colocalization is specific, it should occur with cytoskeletal networks in both control and cytochalasin D–treated NHEK. We found that ODC appeared to colocalize to a limited extent with the keratin network in control NHEK and more extensively with this network in cytochalasin D–treated NHEK; colocalization with tubulin or actin was not significant. Furthermore, fibroblasts, which do not have a keratin intermediate filament system, did not appear to organize ODC in the perinuclear/nuclear space. Finally, HeLa cells, which are of epithelial origin, have been shown to organize their keratin intermediate filament system in response to P0 expression (Staugaitis *et al.*, 1990). If ODC localization was dependent on an organized keratin intermediate filament system, then induction of P0 in HeLa cells that are stable clones for this expression would cause ODC to take on a perinuclear subcellular localization. This relationship between an organized keratin intermediate filament system and ODC localization was observed using the P0 HeLa cells.

The apparent colocalization of ODC with the keratin filament network asks the question why epithelial cells have two pools of ODC. Levels of active ODC in NHEK are ~10–100 times higher than that in fibroblasts (Ruhl *et al.*, 1994), and polyamine levels are similarly elevated (Hickok and Uitto, 1992). In addition, in the ODC-rich, testosterone-stimulated murine kidney, predominant expression of the ODC gene is in the epithelial cells of the proximal tubule (Jänne *et al.*, 1990). These observations suggest that epithelial cells may normally maintain high ODC levels, presumably to generate high polyamine levels. The latter may be important for maintaining differentiated functions; e.g., in NHEK, polyamines can be used in protein cross-linking to form the keratinocyte cornified envelope (Piacentini *et al.*, 1991). We suggest that colocalization of ODC with the cytoskeleton could serve to "buffer" the amounts of soluble ODC in the cell.

If epithelial cells buffer levels of soluble ODC by reversibly immobilizing a pool of ODC to cytoskeletal complexes, we would expect to identify a pool of ODC in NHEK that was extractable with the insoluble material. The distribution of ODC in keratin-containing cells was consistent with this model, with a pool of active ODC in soluble and insoluble protein fractions, as determined by two fractionation procedures. In addition, the amounts of active ODC that could be measured in the insoluble fractions could be greatly increased by mechanical disruption. Finally, fibroblasts that showed no evidence of a distinct subcellular localization for ODC also did not exhibit a similar partitioning of ODC between soluble and insoluble fractions. These observations are consistent with the idea that the pool of ODC that fractionates with the insoluble materials is associated with NHEK-specific proteins, e.g., keratin. It should be noted that these findings are different from and we suspect complementary to those described by Heiskala *et al.* (1999). They reported a membrane localization for ODC in fibroblasts that had been treated with TPA, and we have observed a similar localization for ODC in NHEK treated with TPA as noted in Pomidor *et al.* (1995). The possibility of membrane localization was questioned early in our studies. However, on the basis of results with Fractionation Procedure I (Lenk *et al.*, 1977) in which membrane proteins should be extracted

in the Triton X-100 or in the Tween 20 and DOC fractions, we thought it unlikely that a membrane localization could explain the staining and the fractionation profiles that we observed. On the basis of the data published by Heiskala *et al.* (1999), the percentage of ODC localized to the membrane in their system appears to be smaller than the pool cofractionating with the NHEK-insoluble cellular material. Furthermore, Heiskala *et al.* (1999) have suggested that their subset of membrane-associated ODC may in fact be on the actin cytoskeleton. We cannot rule out that an additional small pool of ODC was solubilized when actin was extracted from the cells. However, our data strongly suggest that the majority of the ODC that is measured in the insoluble fractions copartitions with keratin and associated insoluble proteins.

In rat fibroblastic cells, localization of ODC to the plasma membrane after stimulation by TPA appeared to be mediated by a "phox"-like phosphorylation site present in the ODC protein; the presence of this sequence appears to be necessary for cellular transformation (Heiskala *et al.*, 1999). ODC has many additional phosphorylation sites with serine-303 the major site phosphorylated in vitro with casein kinase II and in COS-1 cells transfected with ODC expression plasmids (Rosenberg-Hasson *et al.*, 1991). Phospho-ODC has been purified from RAW264-transformed macrophages using high-salt elution (200 mM NaCl) (Reddy *et al.*, 1996). Although the subset of ODC that was extracted from the insoluble cellular material was enriched in the phosphorylated form of ODC, no clear function for the phosphorylation could be assigned. In unpublished experiments, we have attempted to dephosphorylate the insoluble material by treatment with alkaline phosphatase to determine whether ODC is readily extracted from this insoluble fraction. Although some of the time additional ODC activity is measured after dephosphorylation, the results are unpredictable and suggest that regulation of localization is likely to be complex and dependent on more than the phosphorylation state of ODC (our unpublished results).

Finally, what is the physiological significance of localizing a pool of ODC with the cytoskeleton, thus allowing ODC protein levels to remain high? Data from transgenic mice suggest that the effects of ODC overexpression are dependent on the cell type. When the human ODC gene was overexpressed in transgenic mice using an ubiquitous promoter, the mice had notable abnormalities in reproduction and brain function (Halmekytö *et al.*, 1991; Halonen *et al.*, 1993). In contrast, when liver expression was targeted, no significant phenotypic changes were observed, probably because of stringent control of liver polyamine levels (Alhonen *et al.*, 1996). Overexpression of the murine ODC gene under control of the keratin 6 promoter in transgenic mice specifically targeting ODC expression to hair follicle stem cells resulted in an increased frequency of papilloma formation (Megosh *et al.*, 1995; O'Brien *et al.*, 1997). In Balb/MK keratinocytes, ODC overexpression also caused increased activation and nuclear translocation of protein kinase CK2, a serine/threonine protein kinase that may be oncogenic (Shore *et al.*, 1997; Xu *et al.*, 1999). Thus, maintaining ODC at high levels in skin could have especially profound effects on tumor formation.

It is intriguing that, in beginning to elucidate the pathway through which ODC overexpression results in cellular transformation, Hölttä, Andersson, and their groups have found that hyperphosphorylation of $p130^{CAS}$, a src substrate localized to the focal adhesion complex, is a downstream consequence of ODC overexpression (Auvinen *et al.*, 1995) and that transformation is dependent on an intact phox sequence in the ODC (Heiskala *et al.*, 1999). Because the focal adhesion directly tethers actin stress filaments, regulates actin organization, and is an important step in signal transduction cascades (Schaller and Parsons, 1994), it will be of special interest to determine how the changes in cytoskeletal organization that we have observed concomitant with regulation of ODC levels integrate with altered activity of the focal adhesion complex to regulate cell growth and cell adhesion.

ACKNOWLEDGMENTS

The authors thank Yingjie Song and Dr. Alain Mauviel (Thomas Jefferson University) for NHEK cultures, Dr. David Colman (Mt. Sinai School of Medicine) for P0 cells, Dr. Kamel Khalili (Allegheny University of the Health Sciences) for the pur α antibody, Dr. Tom O'Brien (Lankenau Medical Center) for MBP-ODC, and Dr. Lo Persson (University of Lund) for His-ODC. This work was supported by National Institutes of Health grants AR-40022 (N.J.H.), AR-41757 (N.J.H.), and CA-71602 (R.S.T. and N.J.H.) and by grants (O.A.J.) from the Medical Research Council (Academy of Finland), the Finnish Foundation for Cancer Research, and the University of Helsinki. M.M.P. was supported in part by a Smith Fellowship from Thomas Jefferson University.

REFERENCES

Adams, J.C., and Watt, F.M. (1989). Fibronectin inhibits the terminal differentiation of human keratinocytes. Nature *340*, 307–309.

Alexandrova, N., Niklinski, J., Bliskovsky, V., Otterson, G.A., Blake, M., Kaye, F.J., and Zajac-Kaye, M. (1995). The N-terminal domain of c-Myc associates with alpha-tubulin and microtubules in vivo and in vitro. Mol. Cell. Biol. *15*, 5188–5195.

Alhonen, L., Heikkinen, S., Sinervirta, R., Halmekytö, M., Alakuijala, P., and Jänne, J. (1996). Transgenic mice expressing the human ornithine decarboxylase gene under the control of mouse metallothionein I promoter. Biochem. J. *314*, 405–408.

Assoian, R.K., and Zhu, X. (1997). Cell anchorage and the cytoskeleton as partners in growth factor dependent cell cycle progression. Curr. Opin. Cell Biol. *9*, 93–98.

Auvinen, M., Paasinen, A., Andersson, L.C., and Hölttä, E. (1992). Ornithine decarboxylase activity is critical for cell transformation. Nature *360*, 355–358.

Auvinen, M., Paasinen-Sohns, A., Hirai, N., Andersson, L.C., and Hölttä, E. (1995). Ornithine decarboxylase- and ras-induced cell transformations: reversal by protein tyrosine kinase inhibitors and role of $pp130^{CAS}$. Mol. Cell. Biol. *15*, 6513–6525.

Balasundaram, D., Tabor, C.W., and Tabor, H. (1991). Spermidine or spermine is essential for the aerobic growth of *Saccharomyces cerevisiae*. Proc. Natl. Acad. Sci. USA *88*, 5872–5876.

Chang, C.F., Gallia, G.L., Muralidharan, V., Chen, N.N., Zoltick, P., Johnson, E., and Khalili, K. (1996). Evidence that replication of human neurotropic JC virus DNA in glial cells is regulated by the sequence-specific single-stranded DNA-binding protein Pur alpha. J. Virol. *70*, 4150–4156.

Dejana, E., Colella, S., Languino, L.R., Balconi, G., Carvascio, G.C., and Marchisio, P.C. (1987). Fibrinogen induces adhesion, spreading,

and microfilament organization of human endothelial cells in vitro. J. Cell Biol. *104*, 1403–1411.

Fischer, S.M., Lee, M.L., Maldve, R.E., Morris, R.J., Trono, D., Burow, D.L., Butler, A.P., Pavone, A., and Warren, B. (1993). Association of protein kinase C activation with induction of ornithine decarboxylase in murine but not human keratinocyte cultures. Mol. Carcinog. *7*, 228–237.

Franke, W.W., Schiller, D.L., Moll, R., Winter, S., Schmid, E., Engelbrecht, I., Denk, H., Krepler, R., and Platzer, B. (1981). Diversity of cytokeratins. Differentiation specific expression of cytokeratin polypeptides in epithelial cells and tissues. J. Mol. Biol. *153*, 933–959.

Halmekytö, M., *et al*. (1991). Transgenic mice aberrantly expressing human ornithine decarboxylase gene. J. Biol. Chem. *266*, 19746–19751.

Halonen, T., *et al*. (1993). Elevated seizure threshold and impaired spatial learning in transgenic mice with putrescine overproduction in the brain. Eur. J. Neurosci. *5*, 1233–1239.

Heiskala, M., Zhang, J., Hayashi, S.-i., Hölttä, E., and Andersson, L.C. (1999). Translocation of ornithine decarboxylase to the surface membrane during cell activation and transformation. EMBO J. *18*, 1214–1222.

Hickok, N.J., and Uitto, J.J. (1992). Regulation of ornithine decarboxylase gene expression, polyamine levels, and DNA synthetic rates by all-trans-retinoic acid in cultured keratinocytes. J. Invest. Dermatol. *98*, 327–332.

Hietala, O., Dzubow, L., Dlugosz, A.A., Pyle, J.A., Jenney, F., Gilmour, S.K., and O'Brien, T.G. (1988). Activation of human squamous cell carcinoma ornithine decarboxylase activity by guanosine triphosphate. Cancer Res. *48*, 1252–1257.

Hölttä, E., Auvinen, M., and Andersson, L.C. (1993). Polyamines are essential for cell transformation by pp60v-src: delineation of molecular events relevant for the transformed phenotype. J. Cell Biol. *122*, 903–914.

Ingber, D.E., Prusty, D., Sun, Z., Betensky, H., and Wang, N. (1995). Cell shape, cytoskeletal mechanics and cell cycle control in angiogenesis. J. Biomech. *28*, 1471–1484.

Isomaa, V.V., Pajunen, A.E.I., Bardin, C.W., and Jänne, O.A. (1983). Ornithine decarboxylase in mouse kidney. Purification, characterization, and radioimmunological determination of the enzyme protein. J. Biol. Chem. *258*, 6735–6740.

Jänne, O.A., Hickok, N.J., Julkunen, M., Crozat, A., Eisenberg, L., and Melanitou, E. (1990). Androgen regulation of gene expression: studies of ornithine decarboxylase in murine kidney. In: Steroid Receptors in Health and Disease, ed. V. Noudgil, New York: Plenum Press, 119–131.

Kubler, M.-D., Jordan, P.W., O'Neill, C.H., and Watt, F.M. (1991). Changes in the abundance and distribution of actin and associated proteins during terminal differentiation of human epidermal keratinocytes. J. Cell Sci. *100*, 153–165.

Lakshmanan, J. (1979). Involvement of cytoskeletal structures in nerve-growth-factor-mediated induction of ornithine decarboxylase. Biochem. J. *178*, 245–248.

Leinonen, P., Alhonen-Hongisto, L., Laine, R., Jänne, O.A., and Jänne, J. (1987). Human myeloma cells acquire resistance to difluoromethylornithine by amplification of ornithine decarboxylase gene. Biochem. J. *242*, 199–203.

Lenk, R., Ransom, L., Kaufman, Y., and Penman, S. (1977). A cytoskeletal structure with associated polyribosomes obtained from HeLa cells. Cell *10*, 67–78.

Li, J.J., and Deshaies, R.J. (1993). Exercising self-restraint: discouraging illicit acts of S and M in eukaryotes. Cell *74*, 223–226.

Marton, L.J., and Morris, D.R. (1987). Molecular and cellular functions of the polyamines. In: Inhibition of Polyamine Metabolism. Biological Significance and Basis for New Therapies, ed. P.P. McCann, A.E. Pegg, and A. Sjoerdsma, New York: Academic Press, 79–105.

Maxwell, S.A., Ames, S.K., Sawai, E.T., Decker, G.L., Cook, R.G., and Butel, J.S. (1991). SV40 large T antigen and p53 are microtubule-associated proteins in transformed cells. Cell Growth Differ. *2*, 115–127.

Megosh, L., Gilmour, S.K., Rosson, D., Soler, A.P., Blessing, M., Sawicki, J.A., and O'Brien, T.G. (1995). Increased frequency of spontaneous skin tumors in transgenic mice which overexpress ornithine decarboxylase. Cancer Res. *55*, 4205–4209.

Moshier, J.A., Dosescu, J., Skunca, M., and Luk, G.D. (1993). Transformation of NIH/3T3 cells by ornithine decarboxylase overexpression. Cancer Res. *53*, 2618–2622.

O'Brien, T.G., Megosh, L.C., Gilliard, G., and Soler, A.P. (1997). Ornithine decarboxylase overexpression is a sufficient condition for tumor promotion in mouse skin. Cancer Res. *57*, 2630–2637.

O'Brien, T.G., Simsiman, R.C., and Boutwell, R.K. (1976). The effect of colchicine on the induction of ornithine decarboxylase by 12-*O*-tetradecanoyl-phorbol-13-acetate. Cancer Res. *36*, 3766–3770.

Oriol-Audit, C., Hosseini, M.W., and Lehn, J.-M. (1985). "Superpolyamines." Macrocyclic polyamines induce highly efficient actin polymerization. Eur. J. Biochem. *151*, 557–559.

Pawson, T. (1991). Signal transduction in the control of cell growth and development. Trends Genet. *7*, 343–345.

Piacentini, M., Farrace, M.G., Imparato, M., Pinedda, L., and Autuori, F. (1991). Polyamine-dependent post-translational modification of proteins in differentiating mouse epidermal cells. J. Invest. Dermatol. *94*, 694–699.

Pohjanpelto, P., Virtanen, I., and Hölttä, E. (1981). Polyamine starvation causes disappearance of actin filaments and microtubules in polyamine-auxotrophic CHO cells. Nature *293*, 475–477.

Pomidor, M.M., Ruhl, K.K., Zheng, P., Song, Y., Jänne, O.A., Tuan, R.S., and Hickok, N.J. (1995). Relationship between ornithine decarboxylase and cytoskeletal organization in cultured human keratinocytes: cellular responses to phorbol esters, cytochalasins, and α-difluoromethylornithine. Exp. Cell Res. *221*, 426–437.

Reddy, S.G., McIlheran, S.M., Cochran, B.J., Worth, L.J., Bishop, L.A., Brown, P.J., Knutson, V.P., and Haddox, M.K. (1996). Multisite phosphorylation of ornithine decarboxylase in transformed macrophages results in increased intracellular enzyme stability and catalytic efficiency. J. Biol. Chem. *271*, 24945–24953.

Rosenberg-Hasson, R., Strumpf, D., and Kahana, C. (1991). Mouse ornithine decarboxylase is phosphorylated by casein kinase-II at a predominant single location (serine-303). Eur. J. Biochem. *197*, 419–424.

Ruhl, K.K., Pomidor, M.M., Rhim, J.S., Tuan, R.S., and Hickok, N.J. (1994). Posttranscriptional suppression of human ornithine decarboxylase gene expression by phorbol esters in human keratinocytes. J. Invest. Dermatol. *103*, 687–692.

Schaller, M.D., and Parsons, J.T. (1994). Focal adhesion kinase and associated proteins. Curr. Opin. Cell Biol. *6*, 705–710.

Seely, J.E., and Pegg, A.E. (1983). Ornithine decarboxylase (mouse kidney). Methods Enzymol. *94*, 158–161.

Seely, J.E., Pösö, H., and Pegg, A.E. (1982). Purification of ornithine decarboxylase from kidneys of androgen-treated mice. Biochemistry *21*, 3394–3399.

Sexton, C.J., Proby, C.M., Banks, L., Stables, J.N., Powell, K., Navsaria, H., and Leigh, I.M. (1993). Characterization of factors involved in human papillomavirus type 16-mediated immortalization of oral keratinocytes. J. Gen. Virol. *74*, 755–761.

Shore, L.J., Soler, A.P., and Gilmour, S.K. (1997). Ornithine decarboxylase expression leads to translocation and activation of protein kinase CK2 in vivo. J. Biol. Chem. *272*, 12536–12543.

Staugaitis, S.M., Smith, P.R., and Colman, D.R. (1990). Expression of myelin basic protein isoforms in nonglial cells. J. Cell Biol. *110*, 1719–1727.

Watt, F.M., Jordan, P.W., and O'Neill, C.H. (1988). Cell shape controls terminal differentiation of human epidermal keratinocytes. Proc. Natl. Acad. Sci. USA *85*, 5576–5580.

Watt, F.M., Kubler, M.-D., Hotchin, N.A., Nicholson, L.J., and Adams, J.C. (1993). Regulation of keratinocyte terminal differentiation by integrin-extracellular matrix interactions. J. Cell Sci. *106*, 175–182.

Xu, X., Landesman-Bollag, E., Channavajhala, P.L., and Seldin, D.C. (1999). Murine protein kinase CK2: gene and oncogene. Mol. Cell. Biochem. *191*, 65–74.